

Residual Stress Effects in Failure from Flaws

B. R. LAWN* and D. B. MARSHALL

MUCH modern strength analysis of brittle solids is based on a somewhat idealized picture of Griffith flaws, that of a well-defined microcrack driven to instability by an applied tension field distributed uniformly across the ultimate separation plane. However, detailed investigations of specific flaw generation processes suggest that, in general, this picture requires modification.¹ The creation of flaws, even in solids usually regarded as essentially brittle, may involve a limited amount of precursor plastic flow which can produce a highly localized, residual stress field about the flaw center. The "pile-up" models of Stroh²⁻⁴ and Cottrell⁵ are the best known examples of deformation-initiated fracture. In such cases the re-

sidual field can significantly modify the stability of subsequent flaw extension in an applied stress field and thus affect the strength characteristics. However, because of the small scale of the postulated events few attempts have been made to obtain quantitative experimental confirmation of any flaw model on a fracture mechanics basis.

In the present work we report on a flaw system which exhibits residual stress effects which may be measured directly. The system consists of a brittle surface loaded with a sharp indenter. Irreversible deformation beneath the contact generates flaw nuclei⁶ which develop into penny-like "median" cracks,^{7,8} generally on indentation symmetry planes: with a Vickers pyramid indenter, for instance, two mutually orthogonal median cracks develop along the indentation diagonals (Fig. 1(A)). These cracks remain open when the indenter is withdrawn, reflecting a residual tensile field due to the permanent deformation zone.^{9,10} Augmentation of the residual field by tension loading then causes the median crack flaw to propagate toward a critical failure configuration (Fig. 1(B)).

The techniques of indentation fracture mechanics may be readily applied to the system shown in Fig. 1.¹¹ Suppose that crack growth occurs under conditions of mechanical equilibrium, expressed in stress intensity factor notation by $K = K_c$. Then the characteristic crack dimension c_0 corresponding to an indentation load P (Fig.

Received July 5, 1978.

Supported by the Australian Research Grants Committee.

The writers are with the Department of Applied Physics, School of Physics, University of New South Wales, Kensington, N.S.W. 2033, Australia.

*Member, the American Ceramic Society.

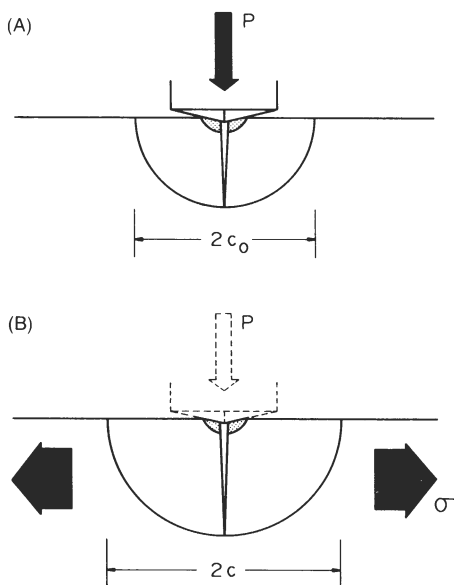


Fig. 1. Fracture mechanics model of deformation-induced median-crack flow system. (A) Sharp indenter at normal load P produces penny-like cracks of characteristic dimension c_0 ; (B) cracks extend to dimension c under combined action of residual indentation field and applied tensile stress σ . (Other crack systems may develop during indentation cycle, but these are not relevant to strength considerations (Ref. 7).)

1(A)) before application of the uniform tensile stress field is given by

$$K = \chi P / c_0^{3/2} = (\chi_e + \chi_r) P / c_0^{3/2} = K_e \quad (1)$$

where the dimensionless constant χ consists of components χ_e due to ideally elastic point loading P at the median crack center (the crack driving force in this case coming from the wedging component of the indentation load normal to the crack plane⁸) and χ_r due to elastic/plastic mismatch stresses about the deformation zone.¹⁰ The component χ_r persists after the indenter is unloaded, so the fracture mechanics relation governing crack growth in an applied tension σ (Fig. 1(B)) becomes

$$K = \chi_r P / c_0^{3/2} + \sigma (\pi \Omega c)^{1/2} = K_e \quad (c \geq c_0) \quad (2)$$

where Ω is another dimensionless constant. There is a strong analogy between the terms in this relation and the corresponding fracture mechanics relation for crack formation in a dislocation pile-up field.¹ Equation (2) transforms into a stress/crack-size function, conveniently normalized, thus

$$\sigma = [K_e / (\pi \Omega c_0)^{1/2}] (c_0/c)^{1/2} [1 - (c_m/c)^{3/2}/4] \quad (c \geq c_0) \quad (3)$$

with a maximum at

$$\sigma_m = 3K_e / 4(\pi \Omega c_m)^{1/2} \quad (4a)$$

$$c_m = (4\chi_r P / K_e)^{2/3} \quad (4b)$$

Note that in the limit of zero residual stress effect, i.e. $\chi_r \rightarrow 0$, $c_m \rightarrow 0$, Eq. (3) reduces to the standard strength equation. Generally, the stability of the indentation flaw depends on the relative values of c_0 and c_m ; Eqs. (1) and (4b) give

$$c_0/c_m = [(1 + \chi_e/\chi_r)/4]^{2/3} \quad (5)$$

so that if $c_0 < c_m$, i.e. if $\chi_r/\chi_e > 1/3$, the flaw extends stably to failure at $\sigma = \sigma_m$, whereas if $c_0 > c_m$, i.e. $\chi_r/\chi_e < 1/3$, the flaw propagates spontaneously at the value of σ given by Eq. (3).

This analysis was tested on soda-lime glass disks, by directly observing median flaw growth under the conditions of Fig. 1(B). The tensile stress was applied biaxially in a symmetrical ring-on-ring flexural arrangement¹² and the resulting flaw extension was followed through an inverted microscope located immediately be-

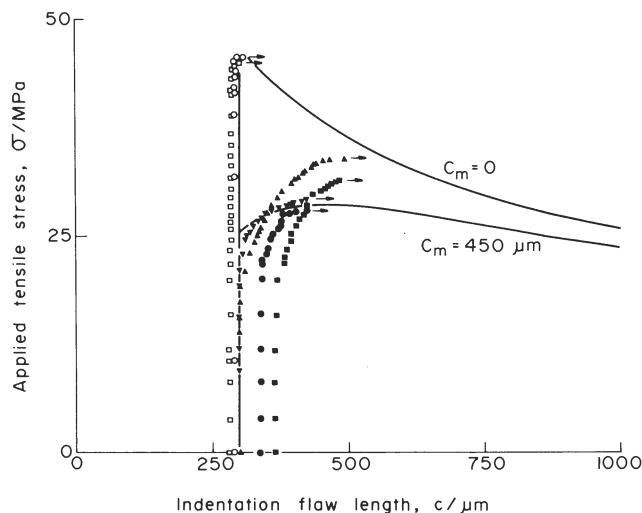


Fig. 2 Equilibrium growth of median-crack flaws to failure (arrowed) in tensile field. Data for soda-lime glass, inert environment, $P = 50$ N, $c_0 = 300$ μm. Each symbol represents a single crack; filled symbols denote as-indented surfaces, open symbols surfaces annealed prior to strength testing. Note initial stable crack growth for $c_0 < c_m$ (producing energy barrier to failure at $\sigma = \sigma_m$) and spontaneous extension to failure for $c_0 > c_m$.

neath the indentation site. To ensure near-equilibrium conditions throughout the test the crack regions were maintained in an inert (moisture-free) environment: the absence of significant flaw extensions over prolonged periods at preselected halt points in the tensile loading provided a check against complications due to slow crack growth. For comparison, tests were run on as-indented specimens ($\chi_r > 0$) and on specimens annealed at 520°C for 24 h immediately after indentation ($\chi_r = 0$).

Test results are plotted as the data points in Fig. 2. The curves in the figure are representations of Eq. (3), fitted to the data with these adjustments: initial flaw size $c_0 = 300$ μm, corresponding to load $P = 50$ N; for annealed disks, $c_m = 0$ and $\sigma = K_e / (\pi \Omega c_0)^{1/2} = 46.9$ MPa at $c = c_0$; and for as-indented disks, $c_m = 450$ μm. These adjustments yield $\chi_r/\chi_e = 0.85$ from Eq. (5) for the as-indented glass surfaces, well in excess of the minimum value specified for the existence of a precursor stage of stable growth prior to failure.

The residual stress term in the present formulation has important implications in the determination of strength properties. Immediately apparent from Fig. 2 is a general lowering of the equilibrium failure stress (cf. similar deleterious effects due to internal stresses in polycrystalline and two-phase ceramics^{13,14}). Perhaps more serious, however, is a prospective acceleration of slow-crack-growth effects in nonequilibrium situations, i.e. in fatigue fracture. Such effects would be expected to enter strongly into stress/lifetime predictions.^{15,16} In terms of Fig. 2, fatigue may be represented by a subcritical path $\sigma(c)$ corresponding to slow growth of the initial indentation flaw toward the unstable branch of the appropriate equilibrium curve. The lifetime at any specified level of stress is then governed by the velocity of the subcritical growth. Various empirical crack-velocity functions have been proposed to describe the fracture kinetics in brittle solids,¹⁷ but the most convenient for present purposes takes the form

$$v = v_0 \exp[B(K/K_e)] \quad (K < K_e) \quad (6)$$

where v_0 and B are constants. Substituting Eqs. (2) and (4b) then gives

$$v = v_0' \exp[B\sigma(\pi \Omega c)^{1/2}/K_e] \quad (K < K_e) \quad (7)$$

which is the standard form for an ideal, residual-stress-free flaw but with

$$v_0' = v_0 \exp[B(c_m/c)^{3/2}/4] \quad (8)$$

replacing v_0 as the preexponential factor. Introducing the residual-stress term into the fracture mechanics therefore effectively in-

creases the crack velocity by a factor $\exp[B(c_m/c)^{3/2}/4]$. For example, at $c = c_m$, using $B = 33$ evaluated from the room temperature data of Wiederhorn and Bolz¹⁸ for soda-lime glass in water, this factor has the value 3.8×10^3 . It is pertinent that v_0'/v_0 has its maximum value at $c = c_0$, i.e. in the region of initial growth which assumes a controlling influence in any lifetime calculations based on ideal-flaw theory.^{15,16} Caution clearly needs to be exercised in ceramics-engineering applications of any design criterion incorporating the ideal-flaw concept, with due regard to the mechanical history of the material under consideration.

¹ B. R. Lawn and T. R. Wilshaw, *Fracture of Brittle Solids*; Ch. 2. Cambridge University Press, London, 1975.

² A. N. Stroh, "Formation of Cracks as a Result of Plastic Flow," *Proc. R. Soc. London, Ser. A*, **223** [1154] 404–14 (1954).

³ A. N. Stroh, "Formation of Cracks in Plastic Flow," *ibid.*, **232** [1191] 548–60 (1955).

⁴ A. N. Stroh, "A Theory of Fracture of Metals," *Adv. Phys.*, **6**[24] 418–65 (1957).

⁵ A. H. Cottrell, "Theory of Brittle Fracture in Steel and Similar Metals," *Trans. AIME*, **212** [3] 192–203 (1958).

⁶ B. R. Lawn and A. G. Evans, "A Model for Crack Initiation in Elastic/Plastic Indentation Fields," *J. Mater. Sci.*, **12** [11] 2195–99 (1977).

⁷ B. R. Lawn and M. V. Swain, "Microfracture Beneath Point Indentations in Brittle Solids," *ibid.*, **10** [1] 113–22 (1975).

⁸ B. R. Lawn and E. R. Fuller, "Equilibrium Penny-Like Cracks in Indentation Fracture," *ibid.*, [12] 2016–24.

⁹ J. J. Petrovic, R. A. Dirks, L. A. Jacobson, and M. G. Mendiratta, "Effects of Residual Stresses on Fracture from Controlled Surface Flaws," *J. Am. Ceram. Soc.*, **59** [3–4] 177–78 (1976).

¹⁰ M. V. Swain, "A Note on the Residual Stress About a Pointed Indentation Impression in a Brittle Solid," *J. Mater. Sci.*, **11** [12] 2345–48 (1976).

¹¹ B. R. Lawn and T. R. Wilshaw, "Indentation Fracture: Principles and Applications," *ibid.*, **10** [6] 1049–81 (1975).

¹² D. B. Marshall and B. R. Lawn, "Strength Degradation of Thermally Tempered Glass Plates," *J. Am. Ceram. Soc.*, **61** [1–2] 21–27 (1978).

¹³ F. F. Lange; pp. 799–819 in *Fracture Mechanics of Ceramics*, Vol. 4, Edited by R. C. Bradt, D. P. H. Hasselmann, and F. F. Lange. Plenum, New York, 1978.

¹⁴ R. W. Rice, S. W. Freiman, R. C. Pohanka, J. J. Mecholsky, Jr., and C. M. Wu; pp. 849–76 in Ref. 13.

¹⁵ S. M. Wiederhorn and A. G. Evans, "Proof Testing of Ceramic Materials—an Analytical Basis for Failure Prediction," *Int. J. Fract.*, **10** [3] 379–92 (1974).

¹⁶ J. E. Ritter, Jr. and J. A. Meisel, "Strength and Failure Predictions for Glass and Ceramics," *J. Am. Ceram. Soc.*, **59** [11–12] 478–81 (1976).

¹⁷ S. M. Wiederhorn; pp. 893–901 in *Fracture 1977*, Vol. 3, Edited by D. M. R. Taplin. University of Waterloo Press, Waterloo, Ontario, Canada, 1977.

¹⁸ S. M. Wiederhorn and L. H. Bolz, "Stress Corrosion and Static Fatigue of Glass," *J. Am. Ceram. Soc.*, **53** [10] 543–48 (1970).